Determination of optic axes by corneal topography among Italian, Brazilian and Chinese populations

Bernardo T Lopes, MD, PhD [1,2], Ashkan Eliasy, MEng, MBA [1], Mohamed Elhalwagy [3], Riccardo Vinciguerra, MD [4], FangJun Bao, MD [5,6], Paolo Vinciguerra, MD [7,8], Renato Ambrósio Jr, MD, PhD [2,9], Ahmed Elsheikh, PhD [1,10,11], Ahmed Abass, PhD [1,12]

[1] Faculty of Science and Engineering, School of Engineering, University of Liverpool, Liverpool, UK
[2] Department of Ophthalmology, Federal University of São Paulo, São Paulo, Brazil
[3] Institute of Translational Medicine, University of Liverpool, UK
[4] Humanitas San Pio X Hospital, Milan, Italy.
[5] School of Ophthalmology and Optometry and Eye Hospital, Wenzhou Medical University, Wenzhou, Zhejiang, China.
[6] Key Laboratory of Vision Science, Ministry of Health, Wenzhou, Zhejiang, China.
[7] Humanitas Clinical and Research Center – IRCCS Rozzano (Mi) – Italy
[8] Humanitas University, Department of Biomedical Sciences, Milan, Italy
[9] Department of Ophthalmology, Federal University the State of Rio de Janeiro (UNIRIO), Rio de Janeiro, Brazil
[10] Beijing Advanced Innovation Center for Biomedical Engineering, Beihang University, Beijing, China
[11] NIHR Biomedical Research Centre for Ophthalmology, Moorfields Eye Hospital NHS Foundation Trust and UCL Institute of Ophthalmology, UK
[12] Department of Production Engineering and Mechanical Design, Faculty of Engineering, Port Said University, Egypt

* Correspondence: blopes@liverpool.ac.uk

Abstract: The study aims to describe a new universal method to identify the relative three-dimensional directions of visual, pupillary and optical axes of the eye and the angles between them using topography elevation data. The method was validated in a large clinical cohort and ethnical differences were recorded. Topography elevation data was collected from 1992 normal eyes of 966 healthy participants in Italy, Brazil and China. The three main axes were defined as follows: optical axis (OA), as that optimal path of light which passes through the ocular system without refraction. The pupillary axis (PA) line was defined using X and Y coordinates of the pupil centre with the chamber depth in addition to the centre of a sphere fitted to the central 3 mm diameter of the cornea. The visual axis (VA) was taken by its best approximation, the coaxially sighted corneal light reflex. The alpha angle was measured between the VA and the OA and the kappa angle between the VA and the PA. The average value of kappa and alpha angles was 3.41±2.84° and 6.04±2.43° in the Italian population, 2.6±1.53° and 5.87±2.3° in the Brazilian and 2.09±1.22° and 3.85±1.48° in the Chinese.

Keywords: cornea; topography; optical axis; visual axis; pupillary axis; kappa angle; alpha angle;

1. Introduction

As the human eye can be considered as a non-aligned optical system [1, 2], a number of theoretical and experimental axes exist which can be used to relate eye alignment and visual performance [3]. Among many other reasons of this non-alignment, the temporal location of the fovea and the relative nasal pupil deviation are of great importance. This led to the presence of three main distinct axes; the visual, the optical and the pupillary axes [4]. The visual axis is the line that passes through the fixation point, front nodal point, rear nodal point and fovea of the eye [5], whereas, the line that passes through the centre of entrance pupil while normal to the corneal surface is defined as a pupillary axis. Finally, the optical axis is the line that passes through the central corneal and stays normal to its surfaces [6]. In theory, it is comparable to the path of a light ray that enters

and leaves the optical system of the eye along the same line [7]. The difference between the visual and the pupillary axes forms the kappa angle (κ) and between the visual and optical axes forms the alpha angle (α) [8].

It is known that the existence of these misalignments leads to optical aberrations that are balanced to improve the retinal image either by different optical elements in the eye or by the incidence angle of the light rays [1, 9]. However, the new customized laser refractive surgery and the implants of multifocal intraocular lenses (IOL) disrupt this balance, these new treatments need to be properly aligned in order to provide the perfect vision for patients [10, 11].

The determination of these axes is challenging due to the absence of appropriate landmarks; therefore, some approximations must be done. The closest measurable point to the visual axis is the coaxially sighted corneal light reflex (CSCLR) [4, 10]. However, the centre of the limbus is commonly used as a landmark to the optical axis, the limbus shape is not symmetrical, and its identification requires the acquisition of a sharp image of the anterior eye [12-14]. Additionally, the optical axis line meets the retina nasally below the fovea missing its central sensitive zone [15], which makes it hard to be identified clinically [16]. Some new topographers and tomographers automatically measure the kappa angle ($\varkappa$) [17-19]. But just a few measures the alpha angle whose importance for IOL planning has been increasingly debated [20]. In brief, the optical centre of the IOL is generally positioned at the centre of the capsular bag, which is placed on the optical axis. The higher the alpha angle is the greater the chance of visual complaints in these patients [20]. The topographic exam is also affected by the physiological misalignment caused by the kappa angle. The corneal keratoconic pattern can be mimicked in patients with misalignments as small as 5° [21]. Therefore, some of these patients that could benefit from refractive surgery are excluded during preoperative screening by a misdiagnose of ectasia susceptibility [22].

The aim of this study is to introduce a method that allows the identification of three main axes of the eye and the determination of the angles between them. This is done through accurate and systematic procedures that can be applied to all topography machines. This method was validated by clinical data from the continents of South America, Europe and Asia where the variations between the three main axes for three ethnicity groups were studied.

2. Materials and Methods

2.1 Clinical data

The study involved the anonymised records of 343 Italian, 177 Brazilian and 476 Chinese participants selected from referrals to Vincieye Eye Clinic (Milan, Italy), Instituto de Olhos Renato Ambrósio (Rio de Janeiro, Brazil), and the Wenzhou Eye Hospital (Wenzhou, China). The clinical characteristics of participants' eyes as measured by the Pentacam HR software were listed in Table 1.

Clinical topography data has been collected from both eyes of normal participants from three populations in three different countries using the Pentacam HR (OCULUS Optikgeräte GmbH, Wetzlar, Germany). Participants from Italy, Brazil and China with no history of ocular disease, trauma or ocular surgery, were selected. Those with intraocular pressure (IOP) higher than 21 mmHg as measured by the Goldmann Applanation Tonometer were excluded, along with those who wore soft contact lenses less than two weeks before measurement and those who wore rigid gas-permeable (RGP) contact lens less than four weeks before measurements.

Raw Pentacam HR elevation data were used in this study, therefore, it was free of the effect of using any mathematical extrapolation techniques. Using the raw data in this study granted the absence of the effect of any smoothening algorithm that could be embedded in the Pentacam HR software. The raw elevation data were exported in comma-separated values (CSV) format and analysed using custom-built MATLAB ® (MathWorks, Natick, USA) codes written especially for this study.

Table 1. Clinical data and characteristics of participants' eyes as measured by the Pentacam HR

	Italian participants	Brazilian participants	Chinese participants
Participants (eyes)	347 (694)	181 (362)	500 (1000)
Age in years; mean ± SD (min : max)	37.6 ± 13.5 (6 : 106)	35.6 ± 15.8 (10 : 87)	24.2 ± 5.7 (17 : 48)

Clinical features and angles	$\overline{Mean \pm SD}$	$\overline{Min: Max}$	$\overline{Mean \pm SD}$	$\overline{Min: Max}$	$\overline{Mean \pm SD}$	$\overline{Min: Max}$
Minimum corneal thickness (μm)	531±420	404:706	550±33	492:660	535±290	453:620
Flat curvature in the central 3 mm zone K1 (D)	42.3±1.9	36.6:47.8	42.6±1.4	39.4:46.6	42.8±1.4	38.2:48.1
Steep curvature in the central 3 mm zone K2 (D)	44.3±2.9	37.1:51.4	43.8±1.5	40.3:47.9	43.9±1.6	38.6:49.5
Index of Bad D	1.2±0.8	-0.7:3.0	0.4±0.5	-0.9:1.4	1.0±0.6	-0.8:3.0
Kappa angle ($\varkappa$)	3.33±1.97	0.09:12.99	2.60±1.52	0.27:10.26	2.09±1.23	0.07:8.68
Alpha angle (α)	5.60±2.48	0.57:18.77	5.38±1.74	0.57:11.22	4.34±1.30	0.81:8.45

SD: Standard deviation. D: Dioptres. Bad D: final index of Belin Ambrosio display.

2.2 Determination of the optical axis

To determine the corneal optical axis as it defined in the literature as that path of light which goes through the ocular system without refraction, a light raytracing algorithm was coded in MATLAB software then validated graphically via AutoCAD software.

The light ray tracing performance was obtained by simulating parallel light rays directed towards the cornea and refracted through the anterior and posterior surfaces according to Snell's law [23, 24], Figure 1. The incidence angle for each ray in the air, ∅_air, was determined as the angle between the ray and the normal vector to the corneal surface at the point of incidence (Figure 1a). The direction of the refracted ray as it passed through corneal depth, ∅_(cornea_anterior), was calculated by Equation 1. Where the refractive indices of air, n_air, cornea, n_cornea, and aqueous, n_aqueous, were set to 1.0, 1.376 and 1.336, respectively, following Gullstrand's relaxed eye model [23, 25].

$$\emptyset_{cornea\_anterior} = \sin^{-1}\left(\frac{n_{air}}{n_{cornea}}\sin\emptyset_{air}\right) \quad \text{Equation 1}$$

Each light ray refracted by the cornea's anterior surface was then used as an incident ray on the posterior surface with an incidence angle ∅_(cornea_posterior), before being refracted again when it passed through the posterior surface then left with angle ∅_(aqueous) through the aqueous (Equation 2).

$$\emptyset_{aqueous} = \sin^{-1}\left(\frac{n_{cornea}}{n_{aqueous}}\sin\emptyset_{cornea\_posterior}\right) \quad \text{Equation 2}$$

The next step was to locate the point of intersection between the refracted light ray and the corneal longitudinal axis. From this point, the focal length f of each light ray could be

calculated as the distance from this point to the corneal apex. With f determined, the optical power can be calculated as [26]:

$$P = \frac{n_{aqueous}}{f} \quad \text{Equation 3}$$

In this analysis, it was noted that not all rays intersect the corneal axis due to the existence of spherical aberration. In these cases, the closest points on the corneal visual axis to the refracted light rays were taken as the focal points [27].

Since the optical axis is defined as a straight light ray enters and leaves an optical system along the same line [7] without refraction, such that line may be located by two points on the corneal anterior and posterior surfaces. When a light ray penetrates the corneal both surfaces without refraction, the focal length of this line will be infinity and its power will tend towards zero according to Equation 3.

Corneal topography data of each eye was rotated in three dimensions in an optimisation loop while the simulated light rays were kept parallel to themselves towards the cornea.

The optimisation looping procedure was set to end when one of the simulated light rays record an infinite focal length and, as a result, zero optical power. This process was carried out by the Levenberg-Marquardt nonlinear least-squares algorithm (LMA) [28, 29] via the MATLAB Optimisation Toolbox. The LMA algorithm was set to stop the optimisation process when the smallest ray's optical power was below 10^{-20}. The optimisation strategy adopted was to rotate the corneal surfaces around Y-axes and X-axes by angles α_x and α_y, respectively, in order to minimise the optical power of a central light ray then select it as the optimal optical axis. The optimisation process for each eye's topography produced the optimal values of the rotation angles α_x and α_y which can be used to locate the optimal location of the eye's optical axis. The rotation was achieved by the following three rotation matrices [30], where α_z was set to zero.

$$R_x(\alpha_x) = \begin{bmatrix} 1 & 0 & 0 \\ 0 & \cos\alpha_x & -\sin\alpha_x \\ 0 & \sin\alpha_x & \cos\alpha_x \end{bmatrix} \quad \text{Equation 4}$$

$$R_y(\alpha_y) = \begin{bmatrix} \cos\alpha_y & 0 & \sin\alpha_y \\ 0 & 1 & 0 \\ -\sin\alpha_y & 0 & \cos\alpha_y \end{bmatrix} \quad \text{Equation 5}$$

$$R_z(\alpha_z) = \begin{bmatrix} \cos\alpha_z & -\sin\alpha_z & 0 \\ \sin\alpha_z & \cos\alpha_z & 0 \\ 0 & 0 & 1 \end{bmatrix} = \begin{bmatrix} 1 & 0 & 0 \\ 0 & 1 & 0 \\ 0 & 0 & 1 \end{bmatrix} \quad \text{Equation 6}$$

Following the elemental rotation rule, the rotated coordinates of the corneal surface X_r, Y_r and Z_r were calculated as

$$\begin{bmatrix} x_{r1} & x_{r2} & x_{r3} & \dots & x_{rn} \\ y_{r1} & y_{r2} & y_{r3} & \dots & y_{rn} \\ z_{r1} & z_{r2} & z_{r3} & \dots & z_{rn} \end{bmatrix} = \left[R_x(\alpha_x) * R_y(\alpha_y) * R_z(\alpha_z)\right] * \begin{bmatrix} x_1 & x_2 & x_3 & \dots & x_n \\ y_1 & y_2 & y_3 & \dots & y_n \\ z_1 & z_2 & z_3 & \dots & z_n \end{bmatrix} \quad \text{Equation 7}$$

Then the light ray tracing process resumed in the optimisation loop after each rotation. In total, 1992 Pentacam comma-separated values (CSV) input data files were managed with an average processing time of 1.5 hours per file in a 4-core central processing unit (CPU). The 2988 hours of optimisation time were split among 8 computers worked in parallel for 16 days.

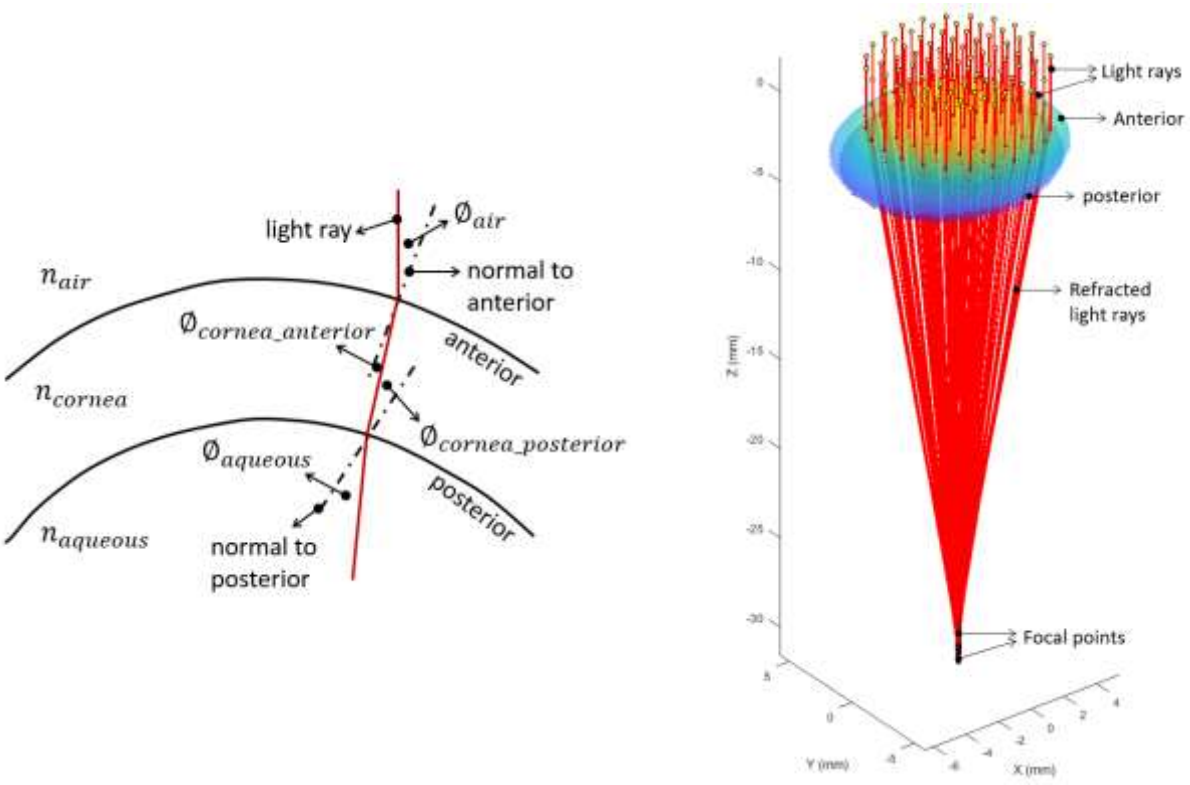

(**a**) (**b**)

Figure 1: Lightray tracing method. (a) Single light ray tracing, (b) Full resolution light ray tracing.

2.3 Determination of the pupillary axis

Following the Cartesian coordinate system, entrance pupil XY centre coordinates data were extracted from the Pentacam elevation CSV files automatically by a custom-built MATLAB code. In order to locate the centre of the entrance pupil back to its natural position, the Pentacam chamber depth value was extracted by the MATLAB code. This value was used to shift the centre of the entrance pupil Z coordinates back to its natural position. The point located by entrance pupil centre XY data and the chamber depth was considered as the first point in the entrance pupil axis. The second point in the entrance pupil axis was calculated by fitting a sphere to the central 3 mm diameter of the cornea, then finding the centre of this sphere. Then by drawing a line passing through the centre of the entrance pupil and the centre of this fitted sphere. This line is representing the pupillary axis, coloured as blue in Figure 2.

2.4 Determination of the visual axis

During scanning the eye with the Pentacam HR Scheimpflug tomographer, the eye becomes oriented in such a way that the coaxially sighted corneal light reflex (CSCLR), which has been demonstrated in theoretical analysis and clinical studies to be the best approximation of the visual axis [10, 31]. It aligns with the tomographer's axis; therefore, the visual axis was taken as the axis of the rotating Pentacam Scheimpflug camera. The intersection of the visual axis with both the corneal surface and the entrance pupil plan were determined as shown in Figure 2 where the visual axis is coloured in green.

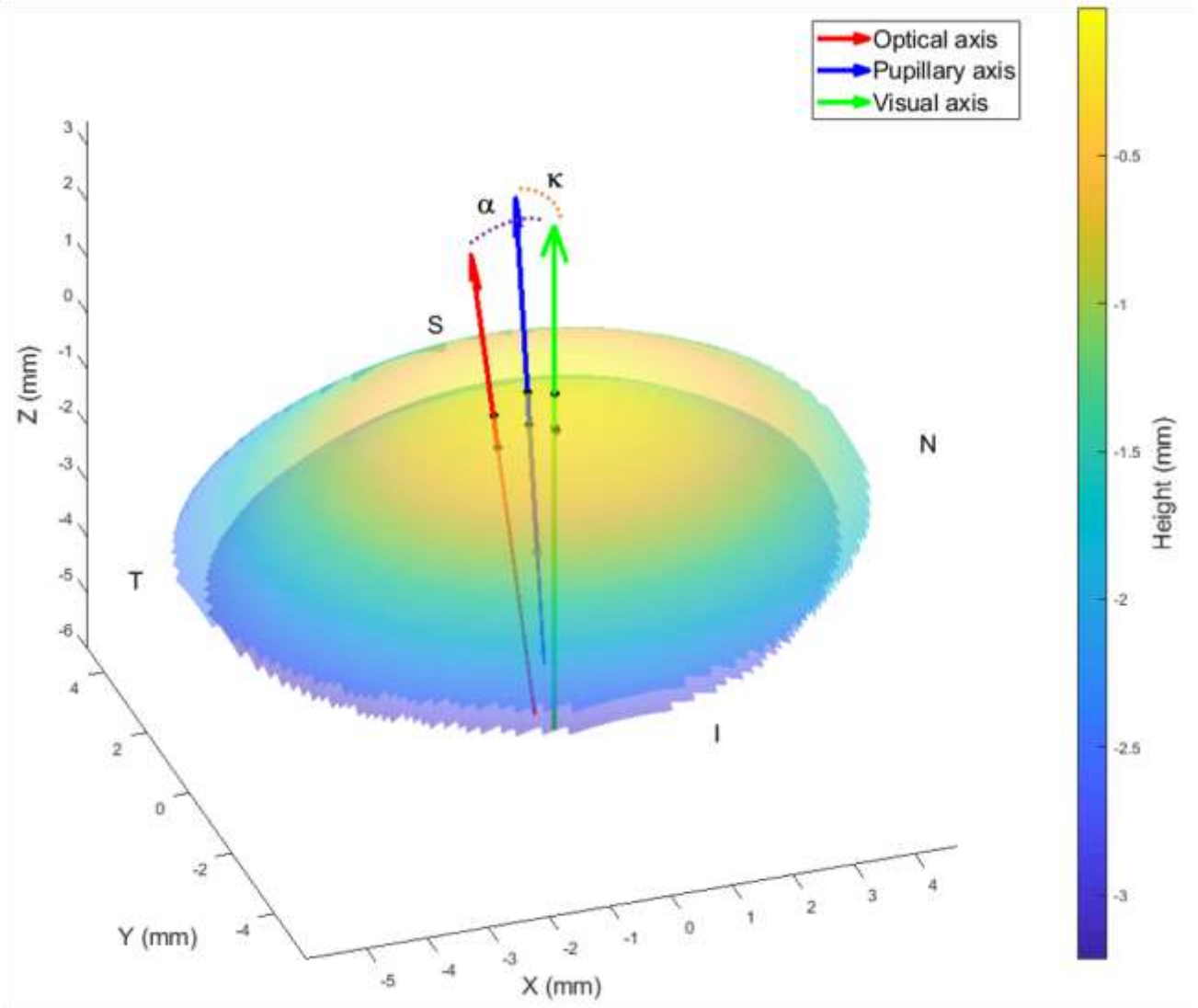

Figure 2: Three-dimension positions of the visual, pupillary and optical axes in a right eye of an Italian participant. N, T, S and I stand for the nasal, temporal, superior and inferior sides of the cornea respectively.

2.5 Statistical analysis

Statistical analysis was performed using MATLAB Statistics and Machine Learning Toolbox (MathWorks, Natick, USA). The null hypothesis probability (p) at 95% confidence level was calculated. Paired and unpaired sample t-tests were used to investigate the significance between samples of data sets to check whether the results represent an independent record. The probability p is an element of the period [0,1] where values of p higher than 0.05 indicate the validity of the null hypothesis [32].

3. Results

A total of 2,056 eyes from 1,028 patients from three different continents was included in this study. The age distribution was different among the groups ($p<0.0001$). The oldest population was from Italy, 37.6 ± 13.5 (6 - 106), followed by the Brazilian, 35.6 ± 15.8 (10 -

87) and the Chinese 24.2 ± 5.7 (17 - 48). Table 1 summarizes the distribution of corneal characteristics among the populations.

The distribution of kappa and alpha angles is summarized in table 2. Regarding the laterality of kappa and alpha angles, the Chinese population presented higher values in the left eye, whilst the Italian and Brazilian population presented higher values in the right eye. Higher differences between the eyes were found in kappa angle. The only statistically significant difference in terms of laterality was present in the kappa angle distribution of the Italian population ($p<0.0001$).

Since the Chinese population was significantly younger, two age groups were defined (less than 20 years and from 20 to 40 years) in order to compare all populations. No statistically significant difference was found between the age groups in the same population. However, there was a slightly decreasing trend in the alpha angle with age for all population. And a slightly increasing trend in the kappa angle for the Brazilian and Chinese population, whilst the Italian group presented the opposite behaviour.

Table 2. The kappa ($\varkappa$) alpha (α) angles distribution between eyes and with age.

	Italian Participants			**Brazilian Participants**			**Chinese Participants**		
Eye side	Right eye Mean±SD Min:Max	Left eye Mean±SD Min:Max	p-value	Right eye Mean±SD Min:Max	Left eye Mean±SD Min:Max	p-value	Right eye Mean±SD Min:Max	Left eye Mean±SD Min:Max	p-value
$\varkappa$ (degree)	3.80 ± 2.04 0.36 : 9.58	2.85 ± 1.76 0.09 : 12.99	<0.001	2.70 ± 1.41 0.34 : 7.31	2.49 ± 1.62 0.27 : 10.27	0.087	2.03 ± 1.24 0.07 : 8.17	2.15 ± 1.22 0.12 : 8.68	0.022
α (degree)	5.64 ± 2.30 0.57 : 14.92	5.55 ± 2.65 0.57 : 18.77	0.518	5.40 ± 1.74 1.03 : 11.22	5.37 ± 1.75 0.57 : 11.18	0.646	4.31 ± 1.28 0.81 : 8.45	4.37 ± 1.31 0.85 : 8.20	0.284
Age Strata	<20 years (n=38) Mean±SD Min:Max	20-40 years (n=356) Mean±SD Min:Max	p-value	<20 years (n=28) Mean±SD Min:Max	20-40 years (n=230) Mean±SD Min:Max	p-value	<20 years (n=328) Mean±SD Min:Max	20-40 years (n=652) Mean±SD Min:Max	p-value
$\varkappa$ (degree)	3.58 ± 1.93 0.94 : 7.95	3.31 ± 1.97 0.09 : 12.99	0.409	2.22 ± 1.53 0.32 : 7.55	2.63 ± 1.52 0.27 : 10.27	0.391	2.00 ± 1.16 0.13 : 7.81	2.14 ± 1.26 0.07 : 8.68	0.501
α (degree)	5.95 ± 2.72 1.92 : 14.92	5.57 ± 2.46 0.57: 18.77	0.418	5.67 ± 1.84 2.23 : 9.39	5.36 ± 1.73 0.57 : 11.22	0.187	4.38 ± 1.25 0.81 : 7.81	4.32 ± 1.32 0.81 : 8.45	0.085

4. Discussion

This study introduced a novel method to determine the main axes of the eye, which can be applied to topographical elevation data from Scheimpflug-based systems. We also evaluated the distribution of the alpha and kappa angles in three different ethnic groups, which may play an important role in certain refractive procedures [10]. These misalignments between the axes of the eye are relevant to ophthalmic surgical procedures and diagnosis. They are increasingly used in clinical practice, but are only available in some commercial devices [17-19], especially the alpha angle [20].

When taking a topographic measurement, the patient aligns their line of sight with the optic axis of the device. Since the fovea is shifted temporally the centre of the map will be slightly nasal. Due to the aspherical shape of the cornea, the peripheral measures present bigger radii than those obtained near the central area. [33] The bigger the distance between the visual axis and the pupillary or the optic axis more distortions on the axial map will be produced. Hubbe and Foulks, did repeated measurements in patients fixating at points progressively further away from the visual axis. In some patients, a deviation of less than 5 degrees produced an asymmetric pattern that mimics keratoconus.[21] The correct determination of the main ocular axes is important to improve the diagnosis of corneal ectatic diseases.

In refractive surgery higher kappa angle values are related with decentred ablation and aggravation of visual symptoms.[34] Reinstein et al. demonstrated that high hyperopic corneal ablations presented similar results in patients with high and low kappa angles, supporting that the entrance pupil centre is not a good landmark for the centration of the procedure and the evaluation of ocular axes is essential for a good surgical outcome.[10]

The correct evaluation of the ocular axes is also fundamental in premium IOL implantation. Prakash et al, observed a positive correlation with visual symptoms after multifocal IOL implantation with preoperative kappa angle values. [11] The alpha angle should also be properly characterized whereas the optical centre of the IOL relies on the centre of the capsular bag which coincides with the optical axis. The higher the value of the alpha angle, more decentred the IOL will be. Roop, proposed a new IOL design where the centre of the lens is nasally shifted producing better optical outcomes experimentally.[20]

Regarding the distribution, the kappa and alpha angles differed among the populations. The Chinese population presented the lowest values (alpha = 4.34 ± 1.30o, kappa = 2.09 ± 1.23o), followed by the Brazilian (alpha = 5.38 ± 1.74o, kappa = 2.6 ± 1.52o) and the Italian (alpha = 5.60 ± 2.48o, kappa = 3.33 ± 1.97o). The overall value of the kappa angle was lower than the ones obtained from different commercial devices reported previously in the literature [17, 18, 35-37]. However, the values of the kappa angle reported differ among different devices [17] and between the topographer and the Synoptophore [18], which exhibit lower values such as the ones reported in this study.

The difference among the population found in our study may rely on the different ethnic background, but also in the different age distribution of the populations, with the Chinese presenting the younger participants. These results are aligned with the ones from Choi and Kim, that observed an increase in kappa angle with age in a Korean population with a mean age of 58.4 years [35].

Gharaee et al, analysed a younger cohort of Iranians from 18 to 45 years. They found a decrease in kappa angle with age in younger patients. Evaluating our results by two different strata of age, below 20 years and between 20 and 40 years, the trend to decrease the kappa angle value with increasing age, although not statistically significant, was observed in the Italian population but wasn't observed in the Brazilian or the Chinese populations. Regarding the alpha angle, it presented a non-significant mild decrease trend with age in all three populations. This different distribution may be a consequence of different ethnic background.

Some differences were found between right and left eyes. Regarding the alpha angle, none of the studied populations presented a statistically significant difference between the eyes. The kappa angle was higher in the right eye among Italian and Brazilian

participants with statistical significance in the Italian population ($p<0.001$ and 0.087, respectively) and was significantly higher in the left eyes among the Chinese participants ($p=0.022$). There are some conflicting results in the literature in relation to this subject. Basmak et al. reported higher values of kappa angle in the left eye, whilst Gharaee et al. reported the higher values of the kappa angle in the right eye [18, 36]. Some hypotheses may be proposed to explain this difference, such as correlation to eye dominance and facial asymmetries or head posture which may affect the distance from the eye to the topographer and affect the reference angles, but they weren't evaluated in this study and further investigations are needed to clarify this aspect.

5. Conclusions

In conclusion, we proposed and validated the consistency in a big cohort of clinical cases, a new universal method to evaluate the different positions of the ocular axes. Some variations with age and eye laterality were observed among the different groups. Some of the variances may be explained by the difference in the ethnic background of the groups. On average, the younger and the western populations studied, were the ones that presented the higher values in both kappa and alpha angles. This information can help clinicians in preoperative screening.

Author Contributions: "Conceptualization, AA. and AElsheikh.; methodology, AA; formal analysis, BL, AEliasy; data curation, RV,PV,RA,FB.; writing—original draft preparation, BL, AEliasy; writing—review and editing, AA, AElshiekh, ME, RV,PV,RA,FB; supervision, AA. All authors have read and agreed to the published version of the manuscript."

Funding: "This research received no external funding".

Institutional Review Board Statement: "Ethical review and approval were waived for this study, due to the use of fully anonymised secondary clinical data".

Conflicts of Interest: RV, PV, RA and Elsheikh are consults for Oculus Optikgeräte GmbH, Wetzlar, Germany. The remaining authors declare no conflict of interest. The funder had no role in the design of the study; in the collection, analyses, or interpretation of data; in the writing of the manuscript, or in the decision to publish the results.

References

1. Berrio E, Tabernero J, Artal P. Optical aberrations and alignment of the eye with age. J Vis. 2010;10(14). doi: 10.1167/10.14.34. PubMed PMID: 21196516.
2. Keller PR, Saarloos PP. Perspectives on corneal topography: a review of videokeratoscopy. Clinical and Experimental Optometry. 1997;80(1):18-30. doi: doi:10.1111/j.1444-0938.1997.tb04843.x.
3. Douthwaite WA, Pardhan S. Surface tilt measured with the EyeSys videokeratoscope: influence on corneal asymmetry. Investigative ophthalmology & visual science. 1998;39(9):1727-35. Epub 1998/08/12. PubMed PMID: 9699563.
4. Pande M, Hillman JS. Optical zone centration in keratorefractive surgery. Entrance pupil center, visual axis, coaxially sighted corneal reflex, or geometric corneal center? Ophthalmology. 1993;100(8):1230-7. PubMed PMID: 8341507.
5. Harris WF. Nodes and nodal points and lines in eyes and other optical systems. Ophthalmic and Physiological Optics. 2010;30(1):24-42. doi: doi:10.1111/j.1475-1313.2009.00690.x.
6. Schwiegerling JT. Eye axes and their relevance to alignment of corneal refractive procedures. J Refract Surg. 2013;29(8):515-6. doi: 10.3928/1081597X-20130719-01. PubMed PMID: 23909777.
7. Arba Mosquera S, Verma S, McAlinden C. Centration axis in refractive surgery. Eye Vis (Lond). 2015;2:4. doi: 10.1186/s40662-015-0014-6. PubMed PMID: 26605360; PubMed Central PMCID: PMCPMC4655455.
8. Moshirfar M, Hoggan RN, Muthappan V. Angle Kappa and its importance in refractive surgery. Oman Journal of Ophthalmology. 2013;6(3):151-8. doi: 10.4103/0974-620X.122268. PubMed PMID: PMC3872563.
9. Espinosa J, Mas D, Kasprzak HT. Corneal primary aberrations compensation by oblique light incidence. Journal of biomedical optics. 2009;14(4):044003. doi: 10.1117/1.3158996. PubMed PMID: 19725715.
10. Reinstein DZ, Gobbe M, Archer TJ. Coaxially sighted corneal light reflex versus entrance pupil center centration of moderate to high hyperopic corneal ablations in eyes with small and large angle kappa. J Refract Surg. 2013;29(8):518-25. doi: 10.3928/1081597X-20130719-08. PubMed PMID: 23909778.

11. Prakash G, Prakash DR, Agarwal A, Kumar DA, Agarwal A, Jacob S. Predictive factor and kappa angle analysis for visual satisfactions in patients with multifocal IOL implantation. Eye (Lond). 2011;25(9):1187-93. doi: 10.1038/eye.2011.150. PubMed PMID: 21681216; PubMed Central PMCID: PMCPMC3178249.
12. Van Buskirk EM. The anatomy of the limbus. Eye. 1989;3 (Pt 2):101-8. doi: 10.1038/eye.1989.16. PubMed PMID: 2695343.
13. Consejo A, Llorens-Quintana C, Radhakrishnan H, Iskander DR. Mean shape of the human limbus. Journal of cataract and refractive surgery. 2017;43(5):667-72. doi: 10.1016/j.jcrs.2017.02.027. PubMed PMID: 28602330.
14. Consejo A, Llorens-Quintana C, Radhakrishnan H, Iskander DR. Mean shape of the human limbus. J Cataract Refract Surg. 2017;43(5):667-72. doi: https://doi.org/10.1016/j.jcrs.2017.02.027.
15. Yang Q, Cho KS, Chen H, Yu D, Wang WH, Luo G, et al. Microbead-induced ocular hypertensive mouse model for screening and testing of aqueous production suppressants for glaucoma. Investigative ophthalmology & visual science. 2012;53(7):3733-41. Epub 2012/05/19. doi: 10.1167/iovs.12-9814. PubMed PMID: 22599582; PubMed Central PMCID: PMC3390181.
16. Thibos LN, Bradley A, Still DL, Zhang X, Howarth PA. Theory and measurement of ocular chromatic aberration. Vision Research. 1990;30(1):33-49. doi: http://dx.doi.org/10.1016/0042-6989(90)90126-6.
17. Dominguez-Vicent A, Monsalvez-Romin D, Perez-Vives C, Ferrer-Blasco T, Montes-Mico R. Measurement of angle Kappa with Orbscan II and Galilei G4: effect of accommodation. Graefes Arch Clin Exp Ophthalmol. 2014;252(2):249-55. doi: 10.1007/s00417-013-2509-y. PubMed PMID: 24253498.
18. Basmak H, Sahin A, Yildirim N, Papakostas TD, Kanellopoulos AJ. Measurement of angle kappa with synoptophore and Orbscan II in a normal population. J Refract Surg. 2007;23(5):456-60. Epub 2007/05/26. PubMed PMID: 17523505.
19. Qi H, Jiang JJ, Jiang YM, Wang LQ, Huang YF. Kappa angles in different positions in patients with myopia during LASIK. International journal of ophthalmology. 2016;9(4):585-9. doi: 10.18240/ijo.2016.04.19. PubMed PMID: 27162734; PubMed Central PMCID: PMC4853357.
20. Roop, Roop P. Optimizing optical outcomes of intraocular lens implantation by achieving centration on visual axis. Indian journal of ophthalmology. 2017;65(12):1425-7. doi: 10.4103/ijo.IJO_653_17. PubMed PMID: 29208827; PubMed Central PMCID: PMC5742975.
21. Hubbe RE, Foulks GN. The effect of poor fixation on computer-assisted topographic corneal analysis. Pseudokeratoconus. Ophthalmology. 1994;101(10):1745-8. PubMed PMID: 7936573.
22. Doyle SJ, Hynes E, Naroo S, Shah S. PRK in patients with a keratoconic topography picture. The concept of a physiological 'displaced apex syndrome'. The British journal of ophthalmology. 1996;80(1):25-8. PubMed PMID: 8664226; PubMed Central PMCID: PMC505378.
23. Smit G, Atchison DA. The eye and visual optical instruments. Cambridge, UK: Cambridge University Press; 1970.
24. Smith DAG. Optics of the Human Eye. Edinburgh EH13AF: Reed Educational and Professional Publishing Ltd; 2000. 261 p.
25. Vojnikovi Bo, Tamajo E. Gullstrand's Optical Schematic System of the Eye Modified by Vojnikovi & Tamajo. Coll Antropol. 2013;37 (1):41-5.
26. Wang L, Mahmoud AM, Anderson BL, Koch DD, Roberts CJ. Total corneal power estimation: ray tracing method versus gaussian optics formula. Investigative ophthalmology & visual science. 2011;52(3):1716-22. doi: 10.1167/iovs.09-4982. PubMed PMID: 21071742.
27. Welford WT. Aberrations of optical systems: CRC Press, Taylor & Francis; 1986.
28. Guyon F, Riche RL. Least Squares Parameter Estimation and the Levenberg-Marquardt Algorithm: Deterministic Analysis, Sensitivities and Numerical Experiments. France: INSA de Rouen; 1999.
29. BjÓrck A. Numerical Methods for Least Squares Problems. Philadelphia: Society for Industrial and Applied Mathematics; 1996. 408 p.
30. Arvo J. Fast random rotation matrices. In: David K, editor. Graphics Gems III. USA: Academic Press Professional, Inc.; 1992. p. 117-20.
31. Mrochen M, Kaemmerer M, Mierdel P, Seiler T. Increased higher-order optical aberrations after laser refractive surgery: a problem of subclinical decentration. J Cataract Refract Surg. 2001;27(3):362-9. Epub 2001/03/20. PubMed PMID: 11255046.
32. Everitt BS, Skrondal A. The Cambridge Dictionary of Statistics. 4 ed. Cambridge, UK: Cambridge University Press; 2010.
33. Chan JS, Mandell RB, Burger DS, Fusaro RE. Accuracy of videokeratography for instantaneous radius in keratoconus. Optom Vis Sci. 1995;72(11):793-9. PubMed PMID: 8587767.
34. Park CY, Oh SY, Chuck RS. Measurement of angle kappa and centration in refractive surgery. Curr Opin Ophthalmol. 2012;23(4):269-75. doi: 10.1097/ICU.0b013e3283543c41. PubMed PMID: 22569467.
35. Choi SR, Kim US. The correlation between angle kappa and ocular biometry in Koreans. Korean J Ophthalmol. 2013;27(6):421-4. Epub 2013/12/07. doi: 10.3341/kjo.2013.27.6.421. PubMed PMID: 24311927; PubMed Central PMCID: PMCPMC3849305.
36. Gharaee H, Shafiee M, Hoseini R, Abrishami M, Abrishami Y, Abrishami M. Angle Kappa Measurements: Normal Values in Healthy Iranian Population Obtained With the Orbscan II. Iran Red Crescent Med J. 2015;17(1):e17873. Epub 2015/03/13. doi: 10.5812/ircmj.17873. PubMed PMID: 25763261; PubMed Central PMCID: PMCPMC4341357.
37. Hashemi H, KhabazKhoob M, Yazdani K, Mehravaran S, Jafarzadehpur E, Fotouhi A. Distribution of angle kappa measurements with Orbscan II in a population-based survey. J Refract Surg. 2010;26(12):966-71. Epub 2010/02/05. doi: 10.3928/1081597X-20100114-06. PubMed PMID: 20128530.